NONSTEADY-STATE HEAT TRANSFER UPON SHOCK WAVE REFLECTION IN A SHOCK TUBE

V. P. Provotorov and V. V. Ryabov

UDC 533.6.011

In recent years shock tubes have become widely used to study thermo- and gas-dynamic processes in high temperature flows and chemical kinetics. In [1, 2] the possibility of analyzing the thermal boundary layer near the shock tube face was studied to determine the dependence of thermal conductivity of a high-temperature gas upon its temperature. It is also possible, in principle, to use data on flow structure behind a reflected shock wave to study processes of heat transfer to a catalytically active surface.

The basic advantages of the reflected shock-wave method are: 1) the temperature behind the reflected wave is approximately twice as high as behind the incident wave (according to estimates for an ideal gas); 2) the gas behind the reflected wave is practically at rest in the laboratory coordinate system.

Significant limitations of this method are the inhomogeneity of the working gas's thermodynamic state and the brief observation times possible (~100 μsec). Other limitations are related to the presence of a viscous boundary layer on the side wall: spatial inhomogeneity of the parameters behind the incident shock wave, leading to time dependence of the gas parameters ahead of the reflected wave, the complex character of reflected wave interaction with the boundary layer on the side wall of the shock tube, and curvature of the incident shock wave. Detailed studies of the effect of the thermal boundary layer formed on the end wall upon motion of the reflected shock wave were performed in [3, 4].

Before directly considering the flow of the relaxing gas in the thermal boundary layer on the catalytic face surface of the shock tube, it is necessary to analyze carefully the flow behind the reflected shock wave. The flow field in this region in the presence of oscillatory nonequilibrium in CO_2 was studied in [5, 6]. Quantitative estimates of the effect of nonequilibrium chemical reactions in oxygen upon flow structure behind the reflected shock wave were presented in [7, 8]. The basic goal of those studies was establishment of the interrelationship between hydrodynamics and chemical processes. A simple chemical model was used. The studies performed revealed that consideration of the dissociation process makes it necessary to abandon the traditional approach in which pressure behind the reflected wave is assumed constant, independent of time. This established fact [7, 8] permitted the authors of [9] to obtain experimentally based values of the nitrogen dissociation rate constant.

Knowledge of the nonviscous nonequilibrium flow field behind the reflected shock wave permits establishment of external boundary conditions, dependent on time, for the thermal boundary layer near the shock tube face. As has already been noted in [10, 11], the effective catalytic activity of the surface may have a significant effect on the thermal flux to the tube surface and its temperature.

The goal of the present study is to consider heat transfer at the shock tube face with nonequilibrium occurrence of physicochemical processes in the thermal boundary layer. Flow parameters behind incident and reflected shock waves will be calculated. The divergence of the gas state from equilibrium will be evaluated for characteristic ranges of the defining parameters (gas pressure and temperature in the shock wave channel, velocity of the incident shock wave, etc.). A simple model is chosen for the physicochemical processes (dissociation–recombination and exchange reactions in air).

1. Gas Flow Behind the Incident Shock Wave. Let the incident shock wave propagate in an ideal gas with parameters p_1, T_1, $x_{O_2} = 0.21$, $x_{N_2} = 0.79$, $x_{NO} = x_O = x_N = 0$, $\kappa_1 = 1.4$ at constant velocity U_S. Then in a coordinate system fixed to the shock wave front, the basic equations of the strong discontinuity for the shock wave take on the form

Zhukovskii. Translated from Zhurnal Prikladnoi Mekhaniki i Tekhnicheskoi Fiziki, No. 5, pp. 84-91, September-October, 1987. Original article submitted May 12, 1986.

0021-8944/87/2805-0721$12.50

$$\rho_2 v_2 = \rho_1 v_1, \; v = u - U_S; \tag{1.1}$$

$$p_2 + \rho_2 v_2^2 = p_1 + \rho_1 v_1^2; \tag{1.2}$$

$$h_2 + \frac{1}{2} v_2^2 = h_1 + \frac{1}{2} v_1^2; \tag{1.3}$$

$$\rho \frac{d\gamma_i}{dt} = \dot{w}_i, \quad \frac{d}{dt} = v \frac{d}{dx}, \quad \dot{w}_i = \sum_{k=1}^{K} (b_{ki} - a_{ki}) \bar{w}_k; \tag{1.4}$$

$$p = \rho \sum_{i=1}^{\nu} \gamma_i RT, \quad \gamma_i = \frac{x_i}{M}, \quad M = \sum_{j=1}^{\nu} x_j M_j; \tag{1.5}$$

$$h_i = c_{pfi} T + \frac{\theta_{vi} R}{\exp\left(\frac{\theta_{vi}}{T}\right) - 1}, \quad h = \sum_{i=1}^{\nu} h_i \gamma_i, \quad c_{pfi} = \frac{\varkappa_i}{\varkappa_i - 1} R. \tag{1.6}$$

Here ρ, p, T, h, γ_i, R, M, κ, θ_{vi}, and u are the density, pressure, temperature, enthalpy, molar-mass concentration of component i, ideal gas constant, molecular weight, specific heat ratio for "frozen" degrees of freedom, characteristic oscillatory temperature [10], gas velocity in the laboratory coordinate system ($u_1 = 0$); b_{ki} and a_{ki} are stoichiometric coefficients for reaction k.

For air, in place of any two of the relationships of Eq. (1.4) we may use the material balance equations

$$\sum_{i=1}^{\nu} \gamma_i M_i = 1; \tag{1.7}$$

$$\frac{\sum_{i=1}^{\nu} \delta_{[O]i} x_i}{\sum_{j=1}^{\nu} \delta_{[N]j} x_j} = \frac{0{,}21}{0{,}79}, \tag{1.8}$$

where $\delta_{\ell i}$ is the number of atoms of element ℓ in molecule i. Expressions for the reaction rates $\bar{w}_k(\gamma_j, T, \rho)$ are presented in [10]. The system of reactions occurring in the five-component mixture O_2, N_2, NO, O, N and the reaction constants used in the present study are described in [11]. We will note that values of the rate constants for reverse chemical reactions have been found to be in good agreement with the results of theoretical and experimental studies [12].

The system of equations presented can be solved at each point of the flow field behind the incident shock wave with the indicated boundary conditions, under the assumption that dissociation is absent on the shock wave front. For numerical solution of system (1.1)-(1.8) a modified Newton's method with optimal choice of iteration step was used [13]. The iteration process was structured so that subsystem (1.1), (1.2) was iterated separately, followed by the second subsystem (1.3)-(1.8).

2. Approximate Solution for the Reflected Shock Wave. The system of equations of motion of a nonviscous relaxing gas behind the reflected shock wave has the form

$$\frac{\partial \rho}{\partial t} + \frac{\partial \rho u}{\partial x} = 0, \quad \frac{\partial \rho u}{\partial t} + \frac{\partial}{\partial x}(\rho u\, u + p) = 0,$$

$$\frac{\partial}{\partial t}\left[\rho\left(e + \frac{u^2}{2}\right)\right] + \frac{\partial}{\partial x}\left[\rho\left(e + \frac{u^2}{2} + \frac{p}{\rho}\right)u\right] = 0, \quad e = h - \frac{p}{\rho},$$

$$\frac{\partial}{\partial t}(\rho \gamma_i) + \frac{\partial}{\partial x}(\rho \gamma_i u) = \dot{w}_i.$$

On the wall we assume u(0, t) = 0. The boundary conditions on the shock wave front are calculated from Rankine–Hugoniot relationships with consideration of the effect of gas relaxation in the incident shock wave wake and variability of the reflected wave velocity $U_R(x, t)$. In this formulation the problem was solved in [7, 8] by the characteristic method. The results

of the calculations of [8] allowed clarification of a number of characteristic features in the flow of the nonviscous relaxing gas behind the reflected shock wave. The most significant of these is the nonsteady-state nature of the flow, which manifests itself as a growth in pressure and concentration of atomic components, as well as a drop in temperature to their equilibrium values with increasing time. The effect of relatively slow pressure growth was used in [9] to study chemical reaction kinetics in nitrogen.

Since that calculation method (the characteristic method) is on the whole quite cumbersome, in the present study we will propose an approximate numerical method which relies on the assumption of low gas velocities behind the reflected wave ($u_3 \approx 0$). Since the velocity of the reflected wave is unknown, while its direction of propagation is opposite to the direction of the incident wave, it is necessary to use relationships between the values of gas velocity, pressure, and density ahead of and behind the compression discontinuity

$$(u_3 - u_2)^2 = (p_3 - p_2)(1/\rho_2 - 1/\rho_3),$$

which follows from Eqs. (1.1), (1.2). After determining ρ_3 and p_3 the velocity of the reflected wave can be calculated from the continuity equation on the discontinuity

$$U_R = (\rho_3 u_3 - \rho_2 u_2)/(\rho_3 - \rho_2).$$

As the positive velocity direction we choose here the direction from the denser gas to the less dense gas incident on the discontinuity. At the initial moment (after reflection) it is assumed that oscillatory degrees of freedom are not excited within the gas, while its chemical composition corresponds to the unperturbed gas state in the channel ahead of the incident shock wave. We can use the convenient approximate estimate of U_R for an ideal gas presented in [14]:

$$U_R/U_S = \left|\frac{3-\varkappa}{2} u_2/U_S - 1\right|.$$

The method for calculation of the gas state behind the reflected shock wave is then analogous to that used in Sec. 1.

3. Thermal Boundary Layer near the Shock Tube Face. We will consider formation of a thermal boundary layer on an infinite plane obstacle for "normal" incidence and subsequent reflection of a plane shock wave. To a certain degree this will be an applicable model of the thermal boundary layer at the face of the shock tube. The gas state in the layer is determined by the system of parameters:

$$t_0,\ \mu_0,\ \rho_0,\ u_0 = \delta/t_0, \quad \delta = (\mu_0 t_0/\rho_0)^{1/2}, \quad l = U_* t_0, \quad \varepsilon^2 = \mu_0/(\rho_0 U_*^2 t_0),$$
$$p_0 = \rho_0 U_*^2/2,$$

where μ_0, t_0, ρ_0, p_0, δ and ℓ are the characteristic viscosity, time, density, pressure, layer thickness, and length, defined by the characteristic velocity U_* (the velocity of the incident or reflected wave). Below we will treat all these quantities as dimensionless, referenced to their characteristic values. We assume the specific heat at constant pressure c_p is referred to c_{p0}, and the temperature T to $U_*^2/(2c_{p0})$. We will consider a multicomponent system of ν components.

In the near-wall flow region at the shock tube face we can introduce the following scales for the independent variables and functions:

$$t = t^{(1)},\ x = \varepsilon x^{(1)} + \ldots,\ u = \varepsilon u^{(1)} + \ldots,\ T = T^{(0)} + \ldots, \tag{3.1}$$
$$\rho = \rho^{(0)} + \ldots,\ p = p^{(0)} + \ldots,\ \alpha_i = \alpha_i^{(0)} + \ldots$$

If we substitute expansion (3.1) in a system of nonsteady-state one-dimensional Navier–Stokes equations and transform to the limit $\varepsilon \to 0$, we obtain the system of equations of the thermal boundary layer [omitting indices on the terms of Eq. (3.1) below]:

$$\frac{\partial \rho}{\partial t} + \frac{\partial \rho u}{\partial x} = 0,\ \frac{\partial p}{\partial x} = 0,\ \rho \frac{\partial \alpha_i}{\partial t} + \rho u \frac{\partial \alpha_i}{\partial x} = -\frac{\partial j_i}{\partial x} + \dot{w}_i, \tag{3.2}$$

$$\rho c_p \frac{\partial T}{\partial t} + \rho u c_p \frac{\partial T}{\partial x} - \left[\frac{dp}{dt}\right] + \sum_{i=1}^{\nu} j_i c_{pi} \frac{\partial T}{\partial x} + \sum_{i=1}^{\nu} \dot{w}_i h_i = \frac{\partial}{\partial x}\left(\lambda' \frac{\partial T}{\partial x}\right),\ \dot{w}_i = M_i \dot{\bar{w}}_i.$$

We assume that the thermal flux q and diffusion flow j_1 have the form [15]

$$q = -\lambda' \frac{\partial T}{\partial x} + \sum_{k=1}^{\nu} h_k j_k, \quad j_i = -\frac{\mu}{\mathrm{Sc}_i}\left(\frac{\partial \alpha_i}{\partial x} + \alpha_i \sum_{k=1}^{\nu} R_{ik}\frac{\partial \alpha_k}{\partial x} + c_{ti}\frac{\partial \ln T}{\partial x}\right).$$

Here λ', h_k, α_k, Sc_k, and c_{tk} are the thermal conductivity coefficient of the gas mixture, enthalpy, mass concentration, effective Schmidt number, and modified thermodiffusion ratio for component K.

We introduce the flow function ψ with the aid of relationships which satisfy the continuity equation identically:

$$\partial\psi/\partial t = -\rho u, \ \partial\psi/\partial x = \rho.$$

Defining new independent variables

$$t = \tau, \ \eta = \psi/(2t)^{1/2}. \tag{3.3}$$

we have

$$\frac{\partial}{\partial t} = \frac{\partial}{\partial \tau} + \frac{\partial \eta}{\partial t}\frac{\partial}{\partial \eta}, \quad \frac{\partial}{\partial x} = \frac{\partial \eta}{\partial x}\frac{\partial}{\partial \eta},$$
$$\rho\frac{\partial}{\partial t} + \rho u\frac{\partial}{\partial x} = \rho\frac{\partial}{\partial \tau} - \frac{\rho\eta}{2\tau}\frac{\partial}{\partial \eta}, \quad \frac{\partial}{\partial x} = \frac{\rho}{(2\tau)^{1/2}}\frac{\partial}{\partial \eta}.$$

After transformations we write system (3.2) as

$$\frac{\partial}{\partial \eta}\left(\frac{c_p N}{\mathrm{Pr}}\frac{\partial T}{\partial \eta}\right) = \sum_{k=1}^{\nu} \hat{j}_k c_{pk}\frac{\partial T}{\partial \eta} - c_p\eta\frac{\partial T}{\partial \eta} + 2\tau\left(\frac{1}{\rho}\sum_{k=1}^{\nu}\dot{w}_k h_k - \frac{1}{\rho}\frac{dp}{d\tau} + c_p\frac{\partial T}{\partial \tau}\right), \tag{3.4}$$
$$-\frac{\partial \hat{j}_i}{\partial \eta} = -\frac{2\tau}{\rho}\dot{w}_i - \eta\frac{\partial \alpha_i}{\partial \eta} + 2\tau\frac{\partial \alpha_i}{\partial \tau}, \quad p = \frac{\rho RT}{M},$$

where

$$N = \rho\mu, \quad \hat{q} = -\frac{c_p N}{\mathrm{Pr}}\frac{\partial T}{\partial \eta} + \sum_{k=1}^{\nu} h_k \hat{j}_k, \tag{3.5}$$
$$\hat{j}_i = -\frac{N}{\mathrm{Sc}_i}\left(\frac{\partial \alpha_i}{\partial \eta} + \alpha_i\sum_{k=1}^{\nu} R_{ik}\frac{\partial \alpha_k}{\partial \eta} + c_{ti}\frac{\partial \ln T}{\partial \eta}\right).$$

The boundary conditions at the outer limit of the thermal boundary layer as $\eta \to \infty$ have the form

$$T = T_\infty(t), \ \alpha_i = \alpha_{i\infty}(t).$$

Values of T_∞, $\alpha_{i\infty}$ were determined by solution of the problem of nonviscous flow of a gas behind the reflected shock wave (see Sec. 2). In the same manner the distribution p = p(t) can be determined.

To find the component concentrations on the free surface of the shock tube ($\eta = 0$) we specify the boundary conditions

$$\sum_{i=1}^{\nu}\delta_{li} j_i = 0 \quad (l = 1, \ldots, \nu_e - 1),$$
$$j_i + k_{wi}\rho\alpha_i = 0 \quad (i = \nu_e, \ldots, \nu - 1), \ \sum_{i=1}^{\nu}\alpha_i = 1.$$

Here $\delta_{\ell i}$ is the number of atoms of element ℓ in component i; k_{wi} is the catalytic recombination rate for component i; ν_e is the total number of chemical elements in the gas mixture considered.

We obtain a boundary condition for temperature on the body surface from the union condition (for temperature and thermal flux). Let heat propagation in the body be described

by the equation $\rho_b c_b \partial T/\partial t = k_b \partial^2 T/\partial y^2$. We will assume that at the initial moment the body is at a temperature T_{00} and that the material temperature at an infinite distance from the face surface remains constant over time $T(\infty, t) = T_{00}$. Then it is simple to find the temperature distribution in the material: $T = c_1[\mathrm{erf}(\beta) - 1] + T_{00}$, $\beta = y/(2\sqrt{at})$, $a = k_b/(\rho_b c_b)$. The union condition takes on the form $T_g = T_{00} - c_1$, $-q_g = -\frac{k_b}{\sqrt{\pi a t}} c_1$, where the subscripts b and g refer to the body material and gas phase, respectively. Transforming to boundary layer variables, we have $T = T_{00} - \varkappa_w \hat{q}$, $\varkappa_w = \sqrt{\frac{\pi a t_0}{2}} \cdot \frac{\rho_0 c_{p\infty} U_* \varepsilon}{k_b}$.

A difference approximation to the system of thermal layer equations (3.1)-(3.7) was constructed in analogy to the method of [16] using a matrix variant of Keller's two-point "box scheme." The method uses second-order approximation for the spatial and time variables. An analysis of stability of the finite difference system for the homogeneous case with constant coefficients was performed in [16] by the spectral method. A variant of the matrix drive method [17] was used to solve the two-point difference equations.

4. Calculation Results. Flow fields behind the reflected shock wave were calculated for incident wave velocity U_S = 5 km/sec and initial pressure $p_1 = 10^2$, 1 Pa (regimes 1 and 2, represented by lines 1 and 2 in Figs. 1-3).

Profiles of nonequilibrium flow parameters behind the incident shock wave are shown in Fig. 1 as functions of distance from the shock wave. The solution obtained is typical of a relaxing dissociated gas. For small times ($t \sim 10^{-8}$ sec) the gas state is close to frozen [18], while at large distances from the shock wave at large times ($t \geq 10^{-5}$ sec) for $p_1 = 10^2$ Pa the flow parameters tend to their limiting equilibrium values [18]. With decrease in initial pressure the equilibrium state is reached at significantly larger distances, while at $t \leq 10^{-5}$ sec the flow parameters differ little from "frozen."

Figure 2 shows temperature T_3 and pressure p_3 on the face wall (in a nonviscous flow) as functions of time. The calculations revealed that approximately 10 μsec after shock wave reflection there begins to form near the end wall a region with constant parameters, the values of which approach equilibrium ones [2, 7]. Two characteristic time scales can be seen. Thus, the parameters which depend upon chemical composition (degree of dissociation, temperature, etc.) relax over a time determined by the chemical reaction rate behind the reflected shock wave. Meanwhile the gas-dynamic parameters (such as pressure, density) relax over a time defined by the time required for establishment of a steady state behind the incident shock wave. Numerous experimental shock tube studies have confirmed these differences [2, 7, 8].

The pressure behind the reflected wave initially falls off somewhat over the course of a brief time interval for regime 1 and an extended time for regime 2, then increases. The initial pressure decrease can be explained by rapid chemical relaxation behind the reflected shock wave [7], which can be seen from the time dependence of temperature T_3. The subsequent growth in pressure p_3 is a consequence of the slower relaxation behind the incident wave. In regime 1 the air flow behind the reflected wave is close to a state of local thermodynamic equilibrium, while in regime 2 it is in a significantly nonequilibrium state.

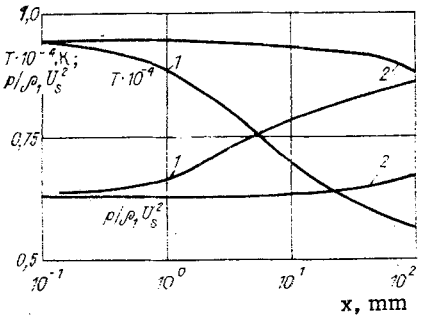

Fig. 1

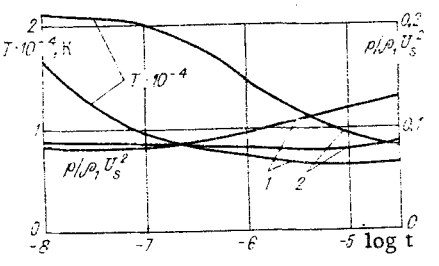

Fig. 2

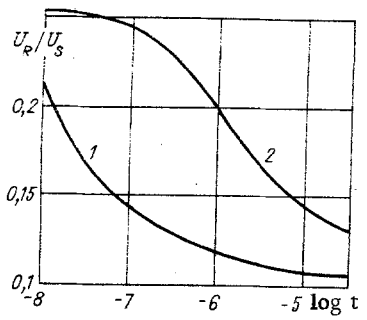

Fig. 3

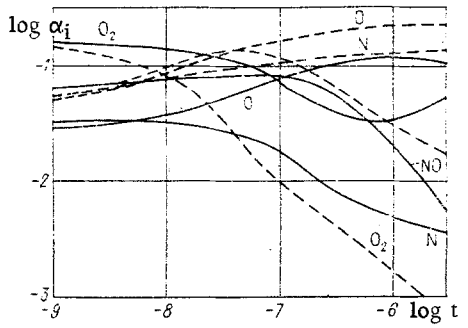

Fig. 4

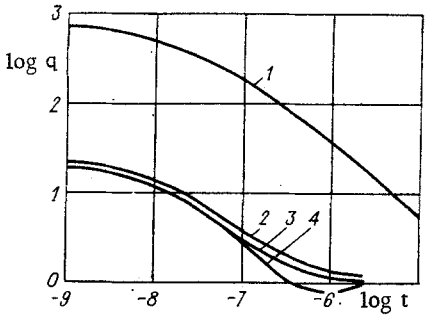

Fig. 5

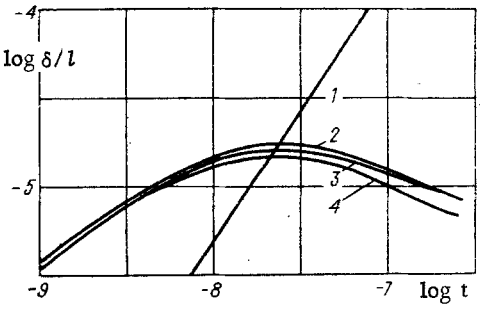

Fig. 6

It was noted above that the dependence $T_3(t)$ determines the relaxation process behind the reflected shock wave. Another quantity, more convenient for experimental verification yet correlating with the temperature dependence, is the velocity of the reflected shock wave. The time dependence of U_R for regimes 1 and 2 is shown in Fig. 3. The general character of the time dependences of T, U_R in both regimes is quite complex. However, as would be expected, with increase in pressure by two orders of magnitude (regime 1), the time required for attainment of the steady state increases by approximately 100 times.

The results presented confirm the possibility of using pressure on the end wall and velocity of the reflected shock wave as parameters to be measured in experiments on chemical kinetics.

We will now turn to analysis of the thermal layer structure. For U_S = 5 km/sec, p_1 = 10^2 Pa, Fig. 4 shows the distributions of component concentrations for air α_i (i = O_2, NO, O, N) at the outer limit of the layer (dashed lines) and a Pyrex end surface (solid lines), with an initial temperature T_{00} = 293 K, as functions of time. The wall material is assumed noncatalytic ($k_{w,O} = k_{w,N} = 1$ cm/sec). At small times (10^{-8} sec $\leq t \leq 10^{-6}$ sec) the thermal layer is intensely nonequilibrium.

Time dependences of thermal flux $q = 2q'/\rho_0 U_S^2$ for various flow regimes and shock tube face materials are shown in Fig. 5. At p_1 = 1 and 10^2 Pa (curves 1 and 4) the thermal flux values at small ($t \sim 10^{-9}$ sec) and large ($t \sim 10^{-6}$ sec) may differ by an order of magnitude. Meanwhile, since for regime 2 at $t \leq 10^{-7}$ sec the thermal layer is in close to a frozen state, the values of q significantly exceed the data for regime 1. At large times the thermal layer state approaches equilibrium for regime 1, while for regime 2 processes within the thermal layer are of a strongly nonequilibrium character near the noncatalytic tube face, as manifests itself in the high thermal flux values for regime 1.* Heating of the face material (Pyrex) to a temperature T_{00} =1000 K (curve 2) or use of another specimen (nickel) at T_{00} = 293 K (curve 3) does not lead to noticeable qualitative changes for $t \leq 0.5$ μsec. For large times the thermal flux values differ by a factor of 2-2.5 times. Significant difficulties arise in obtaining a solution at $t > 2.5$ μsec.

The anomalous behavior of the q(t) functions for relatively large times ($t \geq 0.25$ μsec) is related to the "inhibition" effect of the thermal layer. Figure 6 shows the time develop-

*For a catalytic face material ($k_{w,O}$ = 2200 cm/sec, $k_{w,N}$ = 130 cm/sec) [10] for regime 2, q_w at $t = 10^{-5}$ sec increases by 20%.

ment of thermal layer thickness δ (notation as in Fig. 5). In the cases considered there exist well-defined moments in time at which the layer thickness reaches a maximum. This state, dependent essentially upon the pressure level behind the reflected shock wave and characterized by the value p_1, is produced as a result of abrupt pressure increase behind the reflected shock wave (see Fig. 2). Such a mechanism is possible only in an intensely nonequilibrium gas, where a mechanism acts, which can maintain a positive pressure gradient dp/dt [7]. With increasing t an abrupt reduction occurs in layer thickness, leading to its "inhibition." Unfortunately, within the framework of the present approximate approach it is not possible to establish the complete picture of "viscous–nonviscous interaction."

Thus, the features of the dependence of thermal flux pressure at the shock tube face and reflected shock wave velocity upon time provide valuable information on the characteristics of the thermal viscous layer near the face.

LITERATURE CITED

1. A. Heidon and I. Gerl, The Shock Tube and High-Temperature Chemical Physics [Russian translation], Mir, Moscow (1966).
2. A. B. Britan, "Methods for study of gas thermal conductivity in shock tubes," Report No. 2691, Inst. Mekh. MGU (1983).
3. B. Sturtevant and E. Slachmuylders, "End wall heat-transfer effects on the trajectory of a reflected shock wave," Phys. Fluids, 7, No. 8 (1974).
4. F. A. Goldsworthy, "The structure of a contact region, with application to the reflection of a shock from a heat-conducting wall," J. Fluid Mech., 5, Pt. 2 (1959).
5. D. Baganoff, "Experiment on wall-pressure history in shock–reflexion process," J. Fluid Mech., 23, Pt. 2 (1965).
6. N. H. Johannsen, G. A. Bird, and H. K. Zienkiewicz, "Theoretical and experimental investigations of the reflexion of normal shock waves with vibrational relaxation," J. Fluid Mech., 30, Pt. 1 (1967).
7. Presley and Hanson, "Numerical methods for calculation of flow fields behind a reflected shock wave in a gas with nonequilibrium chemical reactions," Raket. Tekh. Kosmon., 7, No. 12 (1969).
8. R. K. Hanson and D. Baganoff, Shock-Tube Study of Nitrogen Dissociation Rates using Pressure Measurements (AIAA Paper, No. 620), New York (1971).
9. R. K. Hanson, L. L. Presley, and E. V. Williams, Numerical Solutions of Several Reflected Shock-Wave Flow fields with Nonequilibrium Chemical Reactions (NASA Tech. Note, D-6585), Washington (1972).
10. V. P. Agafonov, V. K. Vertushkin, A. A. Gladkov, and O. Yu. Polyanskii, Nonequilibrium Processes in Aerodynamics [in Russian], Mashinostroenie, Moscow (1972).
11. V. P. Provotorov and V. V. Ryabov, "Study of nonequilibrium hypersonic viscous shock layer," Tr. TsAGI, No. 2111 (1981).
12. S. Ch. Lin and J. D. Teare, "Rate of ionization behind shock waves in air, Pt. II. Theoretical interpretations," Phys. Fluids, 6, No. 3 (1963).
13. V. V. Ermakov and N. I. Kalitkin, "The optimal step in Newton's regularization method," Zh. Vychisl. Mat. Mat. Fiz., 21, No. 2 (1983).
14. B. D. Henshell, "Some aspects of shock tube usage in aerodynamic studies," in: Shock Tubes [Russian translation], IL, Moscow (1962).
15. V. V. Ryabov, "Approximate method for calculation of transport coefficients in multicomponent mixtures," Inzh. Fiz. Zh., 44, No. 2 (1982).
16. O. V. Denisenko and V. P. Provotorov, "Study of viscous gas flows in multicomponent mixtures," Tr. TsAGI, No. 2269 (1985).
17. A. A. Samarskii and E. S. Nikolaev, Methods for Solution of Grid Equations [in Russian], Nauka, Moscow (1978).
18. T. V. Bazhenova, L. G. Gvozdeva, Yu. G. Lobastov, et al., Shock Waves in Real Gases [in Russian], Nauka, Moscow (1968).